Applied Physics Letters ARTICLE scitation.org/journal/apl

Ultra-high sensitive trace gas detection based on light-induced thermoelastic spectroscopy and a custom quartz tuning fork

Cite as: Appl. Phys. Lett. **116**, 011103 (2020); doi: 10.1063/1.5129014
Submitted: 24 September 2019 · Accepted: 4 December 2019 ·
Published Online: 7 January 2020

Yufei Ma,[1,a)] Ying He,[1] Pietro Patimisco,[2] Angelo Sampaolo,[2] Shunda Qiao,[1] Xin Yu,[1] Frank K. Tittel,[3] and Vincenzo Spagnolo[2,4]

AFFILIATIONS

[1]National Key Laboratory of Science and Technology on Tunable Laser, Harbin Institute of Technology, Harbin 150001, China
[2]PolySense Lab–Dipartimento Interateneo di Fisica, University and Politecnico of Bari, Via Amendola 173, Bari 70126, Italy
[3]Department of Electrical and Computer Engineering, Rice University, 6100 Main Street, Houston, Texas 77005, USA
[4]State Key Laboratory of Quantum Optics and Quantum Optics Devices, Institute of Laser Spectroscopy, Shanxi University, Taiyuan 030006, China

[a)]Electronic mail: mayufei@hit.edu.cn

ABSTRACT

A highly sensitive trace gas sensor based on light-induced thermoelastic spectroscopy (LITES) and a custom quartz tuning fork (QTF) is reported. The QTF has a T-shaped prong geometry and grooves carved on the prongs' surface, allowing a reduction of both the resonance frequency and the electrical resistance but retaining a high resonance quality factor. The base of the QTF prongs is the area maximizing the light-induced thermoelastic effect. The front surface of this area was left uncoated to allow laser transmission through the quartz, while on the back side of the QTF, a gold film was coated to back-reflect the laser beam and further enhance the light absorption inside the crystal. Acetylene (C_2H_2) was chosen as the target gas to test and validate the LITES sensor. We demonstrated that the sensor response scales linearly with the laser power incident on the prong base, and the optimum signal to noise ratio was obtained at an optical power of 4 mW. A minimum detection limit of ~325 ppb was achieved at an integration time of 1 s, corresponding to a normalized noise equivalent absorption coefficient of 9.16×10^{-10} cm^{-1}W/$\sqrt{\text{Hz}}$, nearly one order of magnitude better with respect to the value obtained with a standard 32.768 kHz QTF-based LITES sensor under the same experimental conditions.

Quartz-enhanced photoacoustic spectroscopy (QEPAS) is one of the most sensitive optical gas sensing techniques.[1] In QEPAS, a quartz tuning fork (QTF) is used as a sensitive acoustic wave transducer. The QTF prongs are deflected by sound waves generated when the gas absorbs modulated light, and subsequently, electrical charges are generated via a direct piezoelectric effect occurring in the quartz. Metal films, such as gold or silver coatings, are deposited on the surface of the QTF and used to collect the generated electrical charge. QEPAS requires that the QTF is installed in a gas chamber containing the target analyte.[2–6] This feature limits the application of QEPAS in some fields, such as remote trace gas detection and combustion diagnostics, in which the detection module needs to be placed far from the sample under investigation. Furthermore, QEPAS is not recommended for detection of corrosive gases, which can compromise the QTF resonance properties (shifts in the resonance frequency, degrading the quality factor due to deterioration of the electrodes and/or the quartz crystal) during long-term exposure.[2,7]

QTFs have been demonstrated acting as detectors to monitor the electromagnetic radiation.[8] A force can be created due to the incident radiation and also produce a torque on the side face of the tuning fork. QTF-based light-induced thermoelastic spectroscopy (LITES)[9,10] is an alternative approach to the QEPAS technique that could overcome the above limitations. In LITES, the laser hits the surface of the QTF and photothermal energy is generated in the crystal because of light absorption by the quartz. Due to the light-thermo elastic conversion, elastic deformations induce a QTF mechanical motion. When the light is intensity-modulated at the resonance frequency of one of the flexural modes of the QTF, the prongs' mechanical vibrations are enhanced and converted into an electrical signal via the piezoelectric effect. The performance of a QTF-based LITES sensor is related to the

absorbed laser energy and the QTF resonance frequency. An optimal laser focusing position on the QTF's surface is the base of QTF's prongs, where high thermally induced stress field can be generated.[9] In this area, the high reflectivity of gold or silver contact layer films normally deposited on the surface of a QTF prevents laser absorption by the quartz crystal. Hence, a special contact pattern design is required to allow and maximize the light absorption. Furthermore, since a custom QTF with a lower resonance frequency is characterized by a longer energy accumulation time, the signal amplitude of LITES is expected to be inversely proportional to the resonance frequency of the QTF and directly proportional to the resonator quality factor. So far, only commercially available QTFs with resonance frequencies >30 kHz (30.72 kHz and 32.768 kHz) have been employed in LITES sensors. Therefore, the implementation of custom QTFs with a low resonance frequency, a high quality factor, and coating pattern properly designed to enhance light absorption by the quartz represents the best way to improve the performance of QTF-based LITES sensors.

In this manuscript, a highly sensitive LITES gas sensor exploiting a low-resonance frequency QTF was demonstrated. A custom T-shaped QTF with carved prong surfaces having a resonance frequency of 9.35 kHz was designed and realized. With respect to QTFs with standard rectangular prongs, T-shaped with a carved surface prong geometry allows the reduction of the resonance frequency and the electrical resistance, while retaining a high quality factor. At the QTF base, where the laser beam is focused, no gold layer was deposited on the front surface in order to allow transmission of the excitation laser beam on the quartz crystal. On the back side, a gold film was coated in order to reflect the transmitted laser beam. In this way, the laser beam passes twice through the quartz crystal, and hence, the local absorption is maximized. Acetylene (C_2H_2) detection is particularly interesting for polyethylene production and electrical arcing fault detection in power transformers.[11,12] Therefore, C_2H_2 was selected as the target gas to test and validate the LITES sensor performance.

The experimental setup of a custom QTF-based LITES sensor is shown in Fig. 1. A distributed feedback (DFB), continuous wave (CW) diode laser with emission at 1530 nm was used as the laser excitation source. A strong C_2H_2 absorption line located at 6534.37 cm^{-1} was selected as the target line. A direct current ramp of the diode laser was used to scan across the absorption line. Wavelength modulation spectroscopy (WMS) and 2nd harmonic (2*f*) detection methods were adopted. Modulation of the laser current was achieved by using a sinusoidal wave. The laser beam emitted from a diode pigtail fiber was collimated by a fiber collimator (FC). The collimated laser beam passed through a 20 cm-long gas cell. At the exit of the absorption cell, a plano–convex lens (L) was employed to focus the laser beam onto the QTF surface. An adjustable attenuator (AA) was installed between the FC and absorption cell to adjust the excitation laser power. The piezoelectric current signal is generated by the QTF because of the light-thermo elastic conversion, and resonance amplification was detected by a transimpedance amplifier (TA) and a lock-in amplifier.

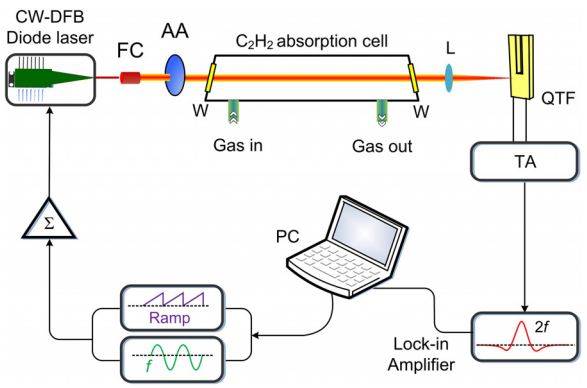

FIG. 1. Schematic diagram of the custom QTF based LITES sensor system.

The optimum resonator for LITES requires long energy accumulation times. Since the accumulation time is proportional to the ratio between the quality factor and the resonance frequency, a reduction of the resonance frequency avoiding a decrease in the quality factor is the key approach. It was demonstrated that to increase the quality factor of the QTF fundamental mode, a reduction of the length of the prongs *L* and an increase in their thickness *T* and of the crystal width are required.[13] On the other hand, the Euler-Bernoulli beam theory shows that the fundamental flexural mode resonance frequency is proportional to T/L^2.[14] This means that a reduction of the resonance frequency may result in a decrease in the quality factor, thus leading to an accumulation time decrease. With the aim to reduce the resonance frequencies and retaining a high quality factor, two different modifications of prong geometry were proposed.[15] The first attempt consisted in a QTF prong geometry with a thickness not constant along the prong axis, but with a T-profile. With respect to the rectangular shape, in the T-shaped QTF, the resonance frequency was reduced by ∼21%, not affecting the quality factor value.[16] The second modification to the standard geometry consisted in carving rectangular 50 μm-deep grooves on the prong surfaces to increase the coupling between the electrodes. With respect to a QTF with uncarved prongs, this approach led to a slight reduction of the resonance frequency (∼4%) and a 36% reduction of the electrical resistance, without affecting the quality factor.[17] These two modifications were finally combined in order to design a T-shaped QTF having rectangular grooves carved on both surface sides, reducing the resonance frequency to 10 kHz and providing a quality factor of ∼10 000 at atmospheric pressure. A schematic of the custom T-shaped QTF is depicted in Fig. 2(a). The rectangular grooves were realized by carving 50 μm of the 250 μm-thick prong surfaces. The small areas between the grooves and the lateral edges of prongs have a width of 100 μm. At the root of QTF's prongs [surface side A in Fig. 2(b)], a 1 mm × 1 mm area was left uncoated to allow

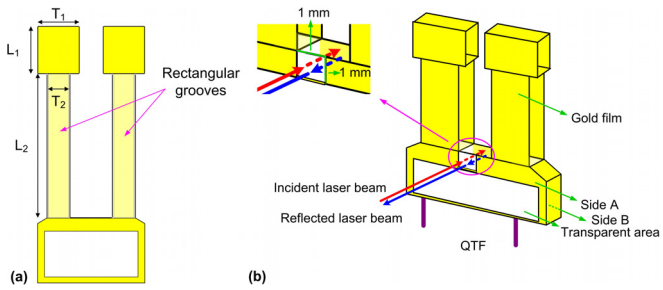

FIG. 2. Schematic diagram of a custom QTF and laser beam. (a) Front view of a T-shaped QTF with rectangular grooves; (b) detailed view of the area selected for laser beam focusing. $T_1 = 2.0$ mm; $T_2 = 1.4$ mm; $L_1 = 2.4$ mm; and $L_2 = 9.4$ mm.

transmission of the incident laser beam. The corresponding backside area [surface side B in Fig. 2(b)] was coated with a gold film having a high reflectivity of ∼98% at 1.53 μm. Thereby, when the laser beam is focused on surface A, it is transmitted through the 250 μm-long quartz crystal thickness and then reflected back by the gold film deposited on surface B. In this way, the light experiences one round trip optical absorption through the crystal. The resonance frequency f_0 and the quality factor Q of the custom QTF were measured by using an electrical excitation method. The QTF resonance curve was $f_0 = 9.35$ kHz and the detection bandwidth $\triangle f = 1.03$ Hz, giving a Q factor of ∼9080, comparable to that of standard 32.7 kHz QTF even though the resonance frequency is more than 3 times lower. Hence, an energy accumulation time larger than 3 times is expected with respect to standard QTF, which is beneficial for the LITES sensor performance.

The dependence of the C_2H_2-LITES sensor performance on laser optical power was investigated. The excitation power from the CW-DFB diode laser was varied in a range from 50 μW to 12.5 mW. The gas cell was filled with a gas mixture of 500 ppm C_2H_2 in nitrogen (N_2), used as the target analyte, and the optimum modulation depth of 0.18 cm^{-1} was adopted.[10] The 2*f* peak signal vs optical power was measured, and the obtained trend is reported in Fig. 3. The experimental data were fitted by a linear function, and the obtained R-square value was 0.99, implying that the C_2H_2-LITES sensor shows an excellent linearity response when the optical power changes in the investigated optical power range. Actually, the signal amplitude of the C_2H_2-LITES sensor was directly proportional to the modulated part of the input radiation. A 2*f* signal waveform with the lowest excitation power of 50 μW is shown in the inset of Fig. 3.

The noise level for the C_2H_2-LITES sensor was measured when the absorption cell was filled with pure N_2. In Fig. 4, the 1σ noise level is reported as a function of the optical power. Up to 2 mW, the 1σ noise level (∼0.4 μV) does not depend on the optical power. As the optical power increases, the 1σ noise level increases and reaches a value of 0.65 μV at 5 mW. At larger power, the 1σ noise level increases much strongly, reaching 3.3 μV at 12.5 mW. Indeed, an increase in the optical power hitting the base of the prong causes an increase in the quartz temperature, which in turn negatively affects the ultimate noise

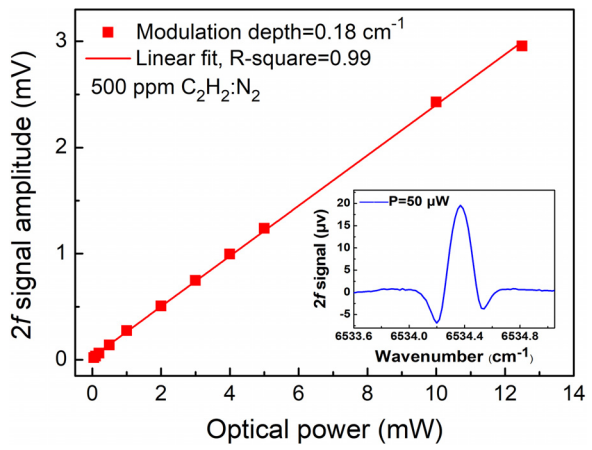

FIG. 3. C_2H_2-LITES 2*f* signal amplitude vs optical power. Inset: 2*f* signal waveform at 50 μW optical power.

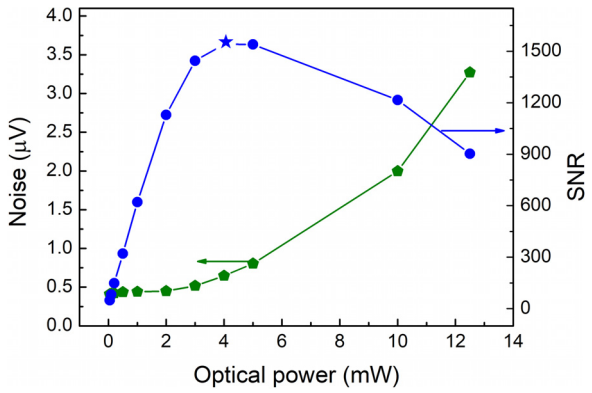

FIG. 4. C_2H_2-LITES noise level and SNR value vs optical power.

level. Hence, the 1σ noise level is dominated by the ultimate thermal noise. The signal-to-noise ratio (SNR) as a function of the optical power was calculated by dividing the 2*f* signal amplitude in Fig. 3 with the 1σ noise values reported in Fig. 4 for each optical power value. The trend of the SNR values vs optical power was also depicted in Fig. 4 (right *y*-axis). As a result, the SNR rapidly increases and reaches the highest value (∼1500) at an optical power of 4 mW and then decreases to 900 at 12.5 mW.

By setting the laser optical power to 4 mW, the response of the custom QTF-based LITES sensor was investigated at different concentrations. The 500 ppm C_2H_2:N_2 gas mixture was diluted with pure N_2 to generate mixtures with different C_2H_2 concentrations in N_2. The 2*f* QEPAS spectral scans measured at 5 different C_2H_2 concentrations are reported in Fig. 5(a). In WMS, with the increase in the trace gas concentration, the enhanced absorption resulted in a more efficient driving of the QTF. Therefore, the signal level of the QTF based LITES sensor increased with the concentration. Based on the HITRAN database, the absorbance for this C_2H_2 absorption line was about 1.1% at the maximum concentration of 500 ppm C_2H_2:N_2. Therefore, the calculated change of amplitude of the driving radiation was about 44 μW at the optimum optical power of 4 mW. The 2*f* signal peak amplitudes are plotted in Fig. 5(b) and linearly fitted, showing that the C_2H_2-LITES sensor has an excellent linear response in the investigated C_2H_2 concentration range. From the linear fit, a minimum detection limit (MDL) of ∼325 ppb was estimated. The corresponding normalized noise equivalent absorption (NNEA) coefficient was calculated to be 9.16×10^{-10} $cm^{-1}W/\sqrt{Hz}$ for the C_2H_2-LITES sensor. A

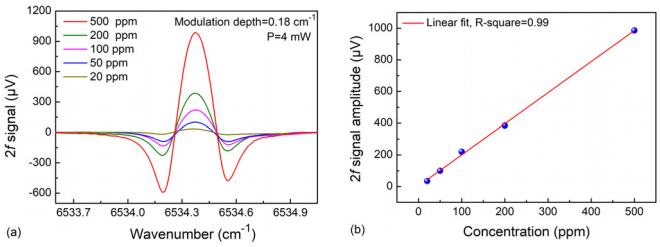

FIG. 5. (a) The concentration response of the custom QTF based LITES signal for an optical power of 4 mW. (b) 2*f* LITES signal amplitude (blue dots) extracted from panel (a) vs C_2H_2 concentrations. The red line represents the best linear fit.

TABLE I. Comparison of the best NNEA achieved for the QTF based C_2H_2 gas sensor using QEPAS and LITES techniques.

	QEPAS[18]	Standard QTF based LITES[10]	Custom QTF based LITES
NNEA ($cm^{-1}W/\sqrt{Hz}$)	4.10×10^{-9}	7.63×10^{-9}	9.16×10^{-10}

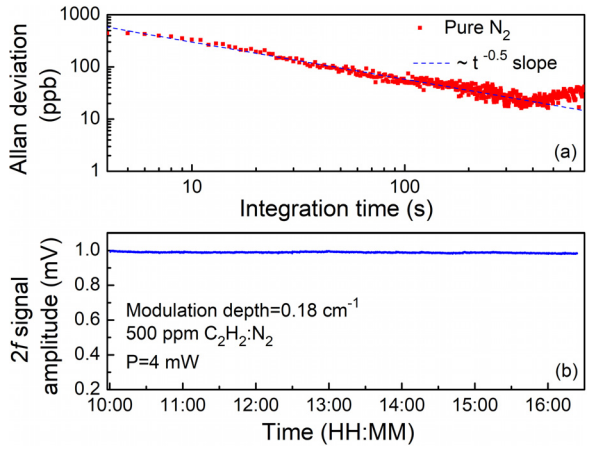

FIG. 6. Long-term measurement for a custom QTF based C_2H_2-LITES sensor system. (a) Allan deviation analysis. (b) Continuous concentration measurement.

comparison with the best NNEA value measured for the standard QTF-based C_2H_2 gas sensor using QEPAS and LITES techniques is shown in Table I. The LITES approach provided an improvement in the gas sensor sensitivity by nearly a factor of 10 with respect to the same configuration employing a standard QTF and 5 times better than the reported best QEPAS result.

The long-term stability of the custom QTF based C_2H_2-LITES sensor system was investigated. In the Allan deviation analysis approach, the absorption cell was flushed with pure N_2 and the experimental result is displayed in Fig. 6(a). The Allan deviation plot follows a $1/\sqrt{t}$ dependence up to an integration time of 370 s, which corresponds to a MDL of 19 ppb. For the continuous concentration measurement, a 500 ppm C_2H_2:N_2 and an optimized optical power of 4 mW were used. As shown in Fig. 6(b), the signal level fluctuation of ~1% in the long-term measurement of more than 6 h indicated that this technique is characterized by an excellent stability.

In this work, we demonstrated a highly sensitive LITES gas sensor based on a custom QTF with a T-shaped prong geometry and rectangular grooves carved on their surfaces. This gives a resonance frequency of the fundamental flexural mode of 9.35 kHz with a quality factor of ~9080, corresponding to a resonator energy accumulation time more than 3 times higher with respect to a standard 32.7 kHz QTF. By uncoating one surface of the area at the base of the QTF's prong, the laser beam passes twice through the quartz crystal, maximizing the light absorption. Employing a 1.53 μm diode laser as the light source and C_2H_2 as the target gas, we demonstrated that the highest signal to noise ratio (SNR) was achieved at an optical power of 4 mW, and the LITES approach provided an improvement in the gas sensor sensitivity by nearly a factor of 10 with respect to the same configuration employing a standard QTF and 5 times better than the best QEPAS result reported to date. At the best operating conditions, a MDL of ~325 ppb was achieved at a 1 s integration time, leading to a NNEA of 9.16×10^{-10} $cm^{-1}W/\sqrt{Hz}$. The Allan deviation analysis shows that the MDL can be reduced to 19 ppb when the integration time is set to 370 s. Furthermore, the long-term concentration investigation indicated that this technique could provide an excellent stability for long-term measurement.

This work was supported by the National Natural Science Foundation of China (Grant Nos. 61875047 and 61505041), Natural Science Foundation of Heilongjiang Province of China (Grant No. YQ2019F006), Fundamental Research Funds for the Central Universities, and Financial Grant from the Heilongjiang Province Postdoctoral Foundation (Grant No. LBH-Q18052). The authors from Dipartimento Interateneo di Fisica di Bari acknowledge the financial support from THORLABS GmbH within the joint-research laboratory PolySense. Frank K. Tittel acknowledges support from the Robert Welch Foundation (Grant No. C0586).

REFERENCES

[1]P. Patimisco, A. Sampaolo, L. Dong, F. K. Tittel, and V. Spagnolo, Appl. Phys. Rev. **5**, 011106 (2018).
[2]H. M. Yi, R. Maamary, X. M. Gao, M. W. Sigrist, E. Fertein, and W. D. Chen, Appl. Phys. Lett. **106**, 101109 (2015).
[3]J. P. Waclawek, H. Moser, and B. Lendl, Opt. Express **24**, 6559 (2016).
[4]K. Liu, X. Y. Guo, H. M. Yi, W. D. Chen, W. J. Zhang, and X. M. Gao, Opt. Lett. **34**, 1594 (2009).
[5]Y. F. Ma, R. Lewicki, M. Razeghi, and F. K. Tittel, Opt. Express **21**, 1008 (2013).
[6]T. Milde, M. Hoppe, H. Tatenguem, M. Mordmüller, J. O'Gorman, U. Willer, W. Schade, and J. Sacher, Appl. Opt. **57**, C120 (2018).
[7]Y. F. Ma, Y. He, X. Yu, C. Chen, R. Sun, and F. K. Tittel, Sens. Actuators, B **233**, 388 (2016).
[8]U. Willer, A. Pohlkütter, W. Schade, J. Xu, T. Losco, R. P. Green, A. Tredicucci, H. E. Beere, and D. A. Ritchie, Opt. Express **17**, 14069 (2009).
[9]Y. He, Y. F. Ma, Y. Tong, X. Yu, and F. K. Tittel, Opt. Lett. **44**, 1904 (2019).
[10]Y. F. Ma, Y. He, Y. Tong, X. Yu, and F. K. Tittel, Opt. Express **26**, 32103 (2018).
[11]I. Khan, Z. Wang, I. Cotton, and S. Northcote, IEEE Electr. Insul. Mag. **23**, 5 (2007).
[12]K. L. Miller, E. Morrison, S. T. Marshall, and J. W. Medlin, Sens. Actuators, B **156**, 924 (2011).
[13]P. Patimisco, A. Sampaolo, V. Mackowiak, H. Rossmadl, A. Cable, F. K. Tittel, and V. Spagnolo, IEEE Trans. Ultrason. Ferroelectr. **65**, 1951 (2018).
[14]P. Patimisco, A. Sampaolo, L. Dong, M. Giglio, G. Scamarcio, F. K. Tittel, and V. Spagnolo, Sens. Actuators, B **227**, 539 (2016).
[15]P. Patimisco, A. Sampaolo, M. Giglio, S. Dello Russo, V. Mackowiak, H. Rossmadl, A. Cable, F. K. Tittel, and V. Spagnolo, Opt. Express **27**, 1401 (2019).
[16]M. Giglio, A. Elefante, P. Patimisco, A. Sampaolo, F. Sgobba, H. Rossmadl, V. Mackowiak, H. Wu, F. K. Tittel, L. Dong, and V. Spagnolo, Opt. Express **27**, 4271 (2019).
[17]S. Li, L. Dong, H. Wu, A. Sampaolo, P. Patimisco, V. Spagnolo, and F. K. Tittel, Anal. Chem. **91**, 5834 (2019).
[18]A. A. Kosterev and F. K. Tittel, SAE Int. J. Aerosp. **1**, 331 (2009).